Disruption of *Sur2*-containing K_{ATP} channels enhances insulin-stimulated glucose uptake in skeletal muscle

William A. Chutkow*, Varman Samuel*, Polly A. Hansen*, Jielin Pu†, Carmen R. Valdivia†, Jonathan C. Makielski†, and Charles F. Burant*‡

*Department of Medicine, University of Chicago, Chicago, IL 60637; and †University of Wisconsin, Madison, WI 53792

Communicated by Donald F. Steiner, University of Chicago, Chicago, IL, July 26, 2001 (received for review June 15, 2001)

ATP-sensitive potassium channels (K_{ATP}) are involved in a diverse array of physiologic functions including protection of tissue against ischemic insult, regulation of vascular tone, and modulation of insulin secretion. To improve our understanding of the role of K_{ATP} in these processes, we used a gene-targeting strategy to generate mice with a disruption in the muscle-specific K_{ATP} regulatory subunit, SUR2. Insertional mutagenesis of the *Sur2* locus generated homozygous null (*Sur2*$^{-/-}$) mice and heterozygote (*Sur2*$^{+/-}$) mice that are viable and phenotypically similar to their wild-type littermates to 6 weeks of age despite, respectively, half or no SUR2 mRNA expression or channel activity in skeletal muscle or heart. *Sur2*$^{-/-}$ animals had lower fasting and fed serum glucose, exhibited improved glucose tolerance during a glucose tolerance test, and demonstrated a more rapid and severe hypoglycemia after administration of insulin. Enhanced glucose use was also observed during *in vivo* hyperinsulinemic euglycemic clamp studies during which *Sur2*$^{-/-}$ mice required a greater glucose infusion rate to maintain a target blood glucose level. Enhanced insulin action was intrinsic to the skeletal muscle, as *in vitro* insulin-stimulated glucose transport was 1.5-fold greater in *Sur2*$^{-/-}$ muscle than in wild type. Thus, membrane excitability and K_{ATP} activity, to our knowledge, seem to be new components of the insulin-stimulated glucose uptake mechanism, suggesting possible future therapeutic approaches for individuals suffering from diabetes mellitus.

Distinct isoforms of the ATP-sensitive potassium channel (K_{ATP}) are expressed in many tissues including pancreatic β cells, striated and smooth muscle cells, and neurons (1, 2). This inwardly rectifying potassium-selective channel is composed of a hetero-octomer of four regulatory SUR subunits and four potassium pore proteins, Kir6.1 or Kir6.2 (3). In β cells SUR1 and Kir6.2 form the K_{ATP} channel that is closed in response to the sulfonylurea hypoglycemic drugs (4), stimulating insulin secretion. In the periphery, SUR2 is the primary regulatory subunit expressed in muscle cells, and it pairs with Kir6.1 in vascular smooth muscle and Kir6.2 in skeletal and cardiac muscle (5). SUR2 undergoes multiple tissue-specific splicing that regulates both its sensitivity to inhibition by nucleotides and its response to pharmacological agents (5, 6). Physiologically, the cardiac K_{ATP} channel apparently functions in repolarizing the membrane in the latter part of the action potential (7). Opening of the K_{ATP} channel during short periods of ischemia protects the heart from subsequent ischemic insults by a process known as ischemic preconditioning (8, 9). The vascular K_{ATP} channel plays a role in regulation of vascular tone, and treatment with agents such as diazoxide and pinacidil, which open the K_{ATP} channel, results in vasodilatation (6). In skeletal muscle, the function of the K_{ATP} channel is less well defined, but it may also be responsible for protection against ischemic damage (10).

Disruption of Kir6.2 in mice results in both β cell failure and an increased responsiveness to injected i.p. insulin with a more pronounced hypoglycemic response than that of wild-type mice (11). The enhanced insulin action in this model could be caused by a direct effect of the disruption of the K_{ATP} channel in peripheral tissues, or to compensation for the progressive β cell failure and subsequent persistent hyperglycemia. In this report, we find that a disruptive mutation of *Sur2* in mice does not result in altered β cell morphology or circulating insulin levels but does lead to an enhanced ability of insulin to increase peripheral glucose disposal by directly increasing the intrinsic insulin responsiveness of skeletal muscle. This result suggests a direct role for the K_{ATP} channel in insulin signaling.

Materials and Methods

***Sur2* Targeting Vector Construction.** PCR-generated genomic fragments were inserted into a positive/negative selection pPNT (7.2 kb) plasmid for targeting vector construction (12): The 5′ arm spanned exons 10–12 (forward: 5′-GAGCGTGGAGGAGACACGAATGAAGGAG-3′; reverse 5′-GCTCTAGAGGCTTCAGGTTGTTTCCACTGGCG-3′). The 3′ arm of homology spanned intron 17 to exon 21 (forward: 5′-TAAACTATCCTGCAGGCAACTAGGGGAGGGAGGGAAGGGGC-3′; reverse 5′-AAGGAAAAAAGCGGCCGCAGGATTCCTTCCTGCATCAAATGATCGCTCAG-3′). PCR products and subcloning products were sequenced to confirm identity and proper orientation.

Generation of *Sur2*$^{+/-}$ ES Cells. Positive/negative selection of ES cells (Genome Systems, St. Louis) transfectants with neomycin resistance was performed by postelectroporation growth in G418 and gancyclovir for 10–12 days. Positive clones for homologous recombination were identified by PCR and confirmed by Southern blot analysis after *Nco*I digestion by using a labeled 800-bp *Nco*I/*Bam*HI genomic fragment probe outside of, and 5′ to, the region of the targeting vector.

Generation of *Sur2*$^{+/-}$ Chimeric and Germ-Line Mice. Animal experimentation was performed according to National Institutes of Health guidelines in the FMI animal facility of the University of Chicago and approved by the Institutional Animal Care and Use Committee. ES cells from two independently targeted *Sur2*$^{+/-}$ generated clones were microinjected into C57BL/6 donor blastocysts, which were then implanted into pseudopregnant CD1 foster mothers (13). Resulting male chimeric mice were bred to CD1 females, and heterozygous *Sur2*$^{+/-}$ mice were interbred or bred to CD1 animals to generate further offspring for phenotypic analysis.

Southern and Northern Blot Analysis. Genomic DNA was isolated from mouse tail clippings via overnight proteinase K digestion as described (14), digested with *Nco*I, resolved on 1% agarose gels, and transferred to nylon membranes. The 800-bp ^{32}P-labeled genomic fragment (5′N/B probe, Fig. 1) was hybridized over-

Abbreviations: GLUT, glucose transporter; K_{ATP} channel, ATP-sensitive potassium channel; Kir6.x, inwardly rectifying K channel; SURx, sulfonylurea receptor.

‡To whom reprint requests should be addressed at: Division of Endocrinology and Metabolism, Department of Internal Medicine, University of Michigan, 1500 E. Medical Center Drive, 3920 Taubman Center, Ann Arbor, MI 48109-0354.

The publication costs of this article were defrayed in part by page charge payment. This article must therefore be hereby marked "*advertisement*" in accordance with 18 U.S.C. §1734 solely to indicate this fact.

 www.pnas.org/cgi/doi/10.1073/pnas.201390398

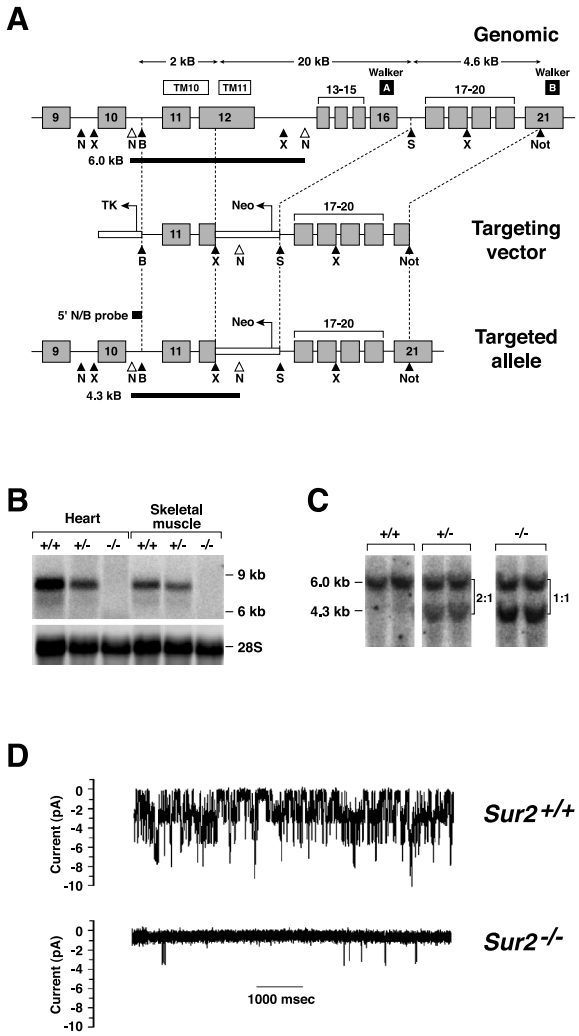

Fig. 1. Generation and evaluation of SUR2 mutant mice. (*A*) Schematic of the mouse *Sur2* targeting strategy. Exons are shaded in gray, and functional motifs are depicted above the exons. TM, predicted transmembrane spanning domain; Neo, neomycin resistance gene; TK, thymidine kinase sequences. Walker A and B motifs are identified as black boxes. Restriction sites are indicated: B, *Bam*HI; N, *Nco*I; S, Sse838; X, *Xba*I. Open triangles, the *Nco*I sites for Southern blot analysis. The probe used for Southern analysis is shown below the targeted allele. (*B*) Northern blot analysis of heart and skeletal muscle for $Sur2^{+/+}$, $Sur2^{+/-}$, and $Sur2^{-/-}$ mice. (*Upper*) Autoradiogram of total RNA probed with a ^{32}P-labeled *Sur2* cDNA probe (bp 0–4231). (*Lower*) Ethidium bromide staining of the 28S ribosomal subunit. (*C*) *Sur2* genotyping. *Nco*I-digested genomic DNA was hybridized with the ^{32}P-labeled probe depicted in the schematic. +/+, wild type; +/−, heterozygote; −/−, homozygote mutant allele. The ratio of the labeled fragment signal intensities for wild-type-to-mutant alleles differentiates heterozygotes (2:1) from homozygotes (1:1). (*D*) Single-channel current recordings in open-cell-attached mode from ventricular myocytes of $Sur2^{+/+}$ (upper tracing) and $Sur2^{-/-}$ (lower tracing). At −40 mV, open current activity is shown as a downward deflection.

night in 5× SSPE [standard saline phosphate/EDTA (0.18 M NaCl/10 mM phosphate, pH 7.4/1 mM EDTA)], 5× Denhardt's solution (0.02% polyvinylpyrrolidone/0.02% Ficoll/0.02% BSA), 0.5% SDS, and single-stranded DNA at 100 μl/ml at 65°C. Labeled fragments were quantitated by PhosphorImaging (Molecular Dynamics). Total RNA was isolated from individual tissues by TRIzol extraction (GIBCO/BRL). RNA (20 μg) was resolved in 1% formaldehyde-agarose gels. Skeletal muscle and heart samples were probed with a ^{32}P-labeled 4,231-bp (0–4231) fragment of SUR2 cDNA or full-length human GLUT4 cDNA.

Western Blot Analysis. Skeletal muscle and cardiac muscle microsomes were prepared as described (15). Microsomal membrane protein was resolved on SDS/10% polyacrylamide gels and transferred to PVDF membranes (Gelman Science, Ann Arbor, MI). Immunoblotting was performed with anti-GLUT4 antibodies (Biogenesis, Bournemouth, U.K.) at 1:1,000 titer, and detected with enhanced chemiluminesence (Pierce).

Serum Chemistry. Whole blood glucose was determined with a Hemocue glucometer (Angelholm, Sweden); serum triglycerides were determined by using a colorimetric assay (Wako Chemicals, Richmond, VA); and insulin concentrations were measured by RIA (Linco Research Immunoassay, St. Louis) with use of rat insulin standards.

Cardiac Myocyte Patch Clamping. Viable ventricular muscle cells were enzymatically isolated from mice 4 months of age by a standard Langendorf perfusion method (16). Voltage clamp methods for K_{ATP} channels were standard as reported (5). The excised inside-out patch method was used with standard solutions with symmetrical 140 mM KCl and 1 μM ATP in the bath.

Intraperitoneal Glucose and Insulin Tolerance Tests. Glucose tolerance tests were performed after a 4-h fast followed by an i.p. injection of glucose at 2 g/kg body mass (2 g/kg). Insulin tolerance tests were performed on postprandial mice by an i.p. injection of 0.5 unit human regular insulin per kg body mass (0.5 u/kg). Blood glucose levels were assayed from tail vein blood.

Hyperinsulinemic Euglycemic Clamp. Clamp studies were performed as described (17). A sterile PE-10 tubing catheter was inserted into the left jugular vein under isoflurane general anesthesia, and externalized through an incision in the skin flap behind the head. On postoperative day 4, after an overnight fast, a 240-min hyperinsulinemic-euglycemic clamp was performed by continuous infusion of regular human insulin at a rate of 15 pmol·kg^{-1}·min^{-1}. Tail vein blood samples were collected at 10-min intervals for the immediate measurement of plasma glucose, and 20% glucose was infused at a varying rate to maintain plasma glucose at basal concentrations of 125 ± 5 mg/dl. Whole body glucose disposal was calculated as the integral of the rate of glucose infusion during the period of blood glucose clamping.

***In Vitro* Glucose Transport Assay.** Glucose transport activity was measured as described (18). Intact soleus muscles, dissected from 8-week-old males, were preincubated for 15 min at 35°C in 2 ml of Krebs–Henseleit bicarbonate buffer, under 5% CO_2. The media were supplemented with 2 mM pyruvate, 0.1% BSA, and either regular insulin at 2,000 microunits/ml or in the absence of insulin. Muscles were transferred to fresh Krebs–Henseleit bicarbonate buffer preincubation buffer with the addition of 0.1 mM 2-[^{3}H]deoxyglucose (0.5 μCi/mmol, Amersham Pharmacia), 0.1 mM [^{14}C]sucrose (0.2 μCi/mmol, Amersham Pharmacia), 0.5 M 2-[^{3}H]deoxyglucose, 50 mM sucrose, and the same insulin concentrations used for sample preincubation, then incubated at 35°C for 15 min. The extracellular space and intracellular 2-[^{3}H]deoxyglucose concentration (micromoles per milliliter of intracellular water) were determined by scintillation counting (19).

Statistical Analysis. Values are reported as mean ± SEM. *P* values were calculated by ANOVA or the Student's *t* test.

Results

Generation of $Sur2^{-/-}$ Mice. Human *SUR1* intron/exon boundaries proved to be highly accurate predictors for the mouse *Sur2* genomic structure with all of the exons preserved between the

PHYSIOLOGY

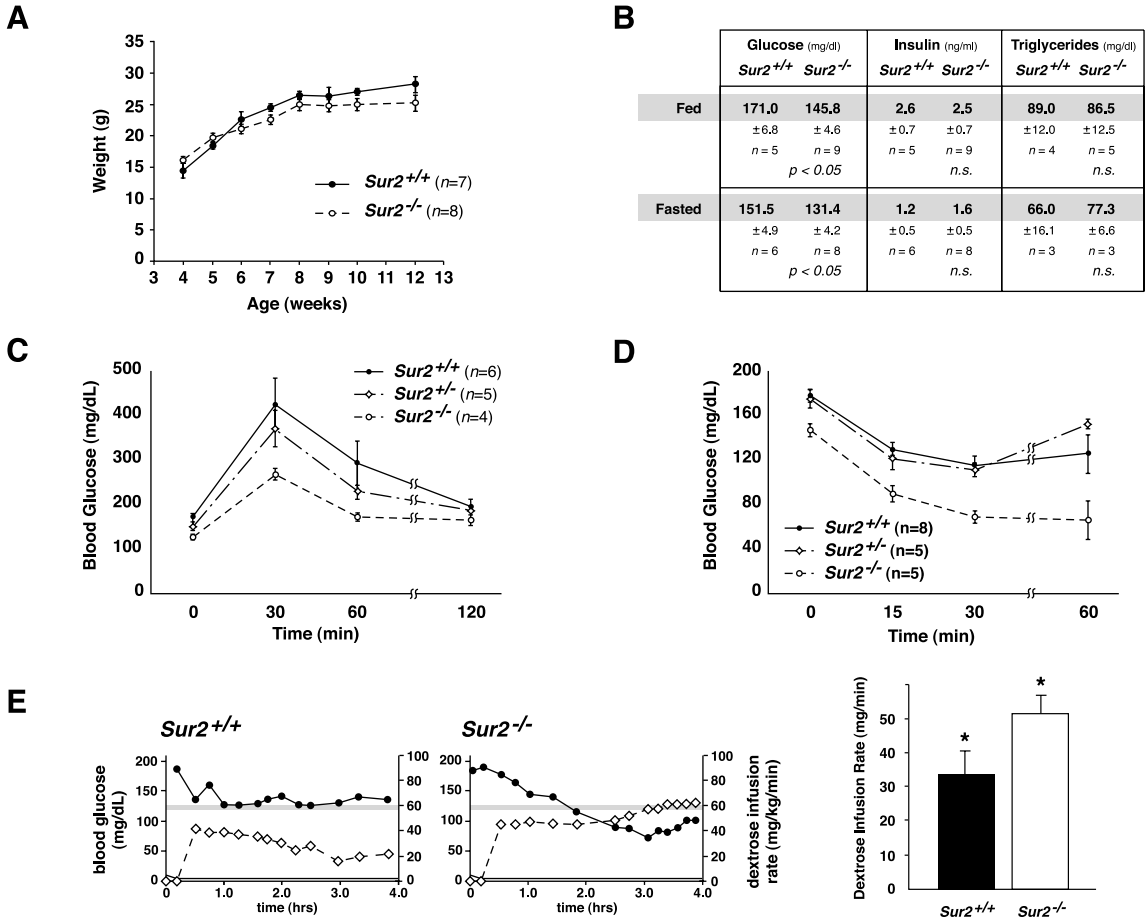

	Glucose (mg/dl)		Insulin (ng/ml)		Triglycerides (mg/dl)	
	Sur2$^{+/+}$	*Sur2*$^{-/-}$	*Sur2*$^{+/+}$	*Sur2*$^{-/-}$	*Sur2*$^{+/+}$	*Sur2*$^{-/-}$
Fed	171.0	145.8	2.6	2.5	89.0	86.5
	±6.8	±4.6	±0.7	±0.7	±12.0	±12.5
	n = 5	*n* = 9	*n* = 5	*n* = 9	*n* = 4	*n* = 5
		p < 0.05		n.s.		n.s.
Fasted	151.5	131.4	1.2	1.6	66.0	77.3
	±4.9	±4.2	±0.5	±0.5	±16.1	±6.6
	n = 6	*n* = 8	*n* = 6	*n* = 8	*n* = 3	*n* = 3
		p < 0.05		n.s.		n.s.

Fig. 2. (*A*) Weight gain in male mice with unrestricted access to standard chow. Weights are expressed as mean values ± SEM. (*B*) Serum glucose, insulin, and triglyceride levels for wild-type and *Sur2*$^{-/-}$ mice between 10 and 12 weeks of age, both in the fasted and fed states. Significance of values between wild-type and *Sur2*$^{-/-}$ mice are indicated. n.s., nonsignificant. (*C*) Response of mice to i.p. injection of glucose (2 g/kg). Serum glucose levels at the indicated time points are expressed as mean values ± SEM (*D*) i.p. insulin tolerance test. Glucose levels were determined in mice injected i.p. with insulin (0.5 U/kg). Values are mean ± SEM (*E*) Representative hyperinsulinemic, euglycemic clamp assays from *Sur2*$^{+/+}$ (*Left*) and *Sur2*$^{-/-}$ (*Right*) mice. Mice were infused with a constant rate of insulin and variable glucose as described in *Materials and Methods*. The closed circles represent the blood glucose levels, and the gray region represents the target blood glucose range. Open diamonds represent the rate of glucose infusion from a 20% glucose solution. A compilation of the rates of glucose infusion is summarized as a bar graph, with an $n = 3$ for *Sur2*$^{+/+}$ mice and an $n = 3$ for *Sur2*$^{-/-}$ (*Right*) mice. *, $P < 0.05$.

two genes and with nearly identical intron/exon boundaries. *Sur2* consists of a minimum of 39 coding exons, the last exon serving as an alternate carboxy-tail variant (20). Previously, we noted two variant sequences in the 5′-untranslated region, suggesting the possibility of alternate transcriptional start sites (1); thus, a "functional knockout" strategy was undertaken. Two arms of homology were generated for the targeting vector that spanned, respectively, intron 10 to exon 12 and intron 17 to exon 21. The deleted domain encompassed the ATP-binding domain of the first nucleotide-binding fold (Walker A motif) and a single predicted transmembrane-spanning domain preceding nucleotide-binding fold 1 (Fig. 1*A*). During F_2 offspring genotyping, it became evident that the original stem cell targeting, from which the founder male developed, had an additional integration event involving a duplication of the *Sur2* locus between exons 9 and 27. The duplicated segment integrated 3′ to the *Sur2* locus as determined by long-range genomic PCR and fluorescence *in situ* hybridization (not shown). However, the native *Sur2* locus was properly targeted and disrupted, because half the amount of mRNA for *Sur2* was found in heart and skeletal muscle of the heterozygous mice and no mRNA was detected for *Sur2* in the homozygous mutant mice (Fig. 2*B*). Sequencing of the 5′ and 3′ targeting boundaries confirmed the proper integration of the targeting vector. Southern blot of *Nco*I-digested genomic DNA from heterozygous mice showed a 6.0-kb fragment (wild-type allele) and a single predicted 4.3-kb mutant allele fragment. The ratio of wild-type to mutant hybridizing intensities is 2:1 as determined by densitometry, which indicates one wild-type allele and a mutant allele that consists of a "wild-type" fragment (the duplicated segment) and the disrupted fragment. Homozygous mutant animals, then, have 1:1 intensity of the mutant 4.3-kb fragment and the 6.0-kb duplicated wild-type segment (Fig. 1*C*). Unambiguous genotyping is thus possible by Southern blotting and by PCR. The absence of K_{ATP} currents in patches isolated from cardiac myocytes (Fig. 1*D*) and skeletal muscle (not shown) confirmed *Sur2* disruption. In 55 patches from cells isolated from three different *Sur2*$^{-/-}$ mice, no K_{ATP} currents were observed. In 23 patches from four different *Sur2*$^{+/-}$mice, K_{ATP} activity was seen in four patches (17%). In 26 patches from wild-type littermates, K_{ATP} currents were detected in 19 patches (74%).

Physiology of *Sur2*$^{+/-}$ and *Sur2*$^{-/-}$ Mice. Homozygous and heterozygous mice showed normal growth until 6 weeks of age, when their weight gain began to lag compared with that of the wild-type animals (Fig. 2*A*). Increased spontaneous mortality in male *Sur2*$^{-/-}$ mice was observed at 6 weeks of age and in females

at 10 weeks of age (W.A.C., J.P., J.C.M., C.F.B., and E. McNally, unpublished work). Serum chemistry, performed on fasted 6- to 8-week-old mice, showed that *Sur2* disruption did not result in changes in serum electrolytes compared with wild-type littermates (data not shown). There was a small but significant decrease in serum glucose levels, although a nonsignificant difference in serum insulin levels, in $Sur2^{-/-}$ mice compared with wild-type controls in both the fasting and fed state (Fig. 2*B*). There was no change in fed or fasting serum triglyceride concentration in male $Sur2^{-/-}$ vs. wild-type mice (Fig. 2*B*).

Assessment of Glucose and Insulin Tolerance. i.p. administration of 2 g/kg of glucose to wild-type mice resulted in a typical increase in glucose levels to a peak of 420 mg/dl. The $Sur2^{+/-}$ mice had identical baseline glucose levels and a relatively normal response to the glucose load. $Sur2^{-/-}$ mice again had decreased fasting glucose concentrations and showed a significantly improved glucose tolerance curve, with peak glucose of ≈250 mg/dl (Fig. 2*C*). To test insulin sensitivity further, wild-type and $Sur2^{-/-}$ mice were challenged with 0.5 U/kg of insulin. Wild-type mice showed a transient decrease in blood glucose, whereas the $Sur2^{-/-}$ mice showed a rapid and sustained reduction in serum glucose, with half the mice either succumbing to hypoglycemia or requiring glucose injections to restore glucose levels (Fig. 2*D*). Again, heterozygous mice, like wild-type mice, showed a typical decrease and rebound in serum glucose after insulin challenge. Whole-body glucose disposal was assessed by an euglycemic, hyperinsulinemic clamp, providing a more discriminating indicator of insulin action. The $Sur2^{-/-}$ mice not only required a greater glucose infusion to maintain target serum glucose levels than wild-type mice did, 51.5 $mg \cdot kg^{-1} \cdot min^{-1}$ vs. 33.9 $mg \cdot kg^{-1} \cdot min^{-1}$, respectively ($P < 0.05$; Fig. 2*E*), but merely maintaining target blood glucose levels proved difficult in $Sur2^{-/-}$ mice, despite a continuously increasing glucose infusion rate.

Insulin Responsiveness in Isolated Skeletal Muscle. The uptake of 2-[^{14}C]deoxyglucose by incubated soleus muscle in the absence of insulin ("basal glucose transport") was not different between $Sur2^{-/-}$ mice and wild-type mice. However, there was a significant 59% increase in glucose uptake after incubation with 2,000 microunits/ml insulin (Fig. 3*A*). There was no change in the levels of GLUT4 mRNA (data not shown) or protein (Fig. 3*B*) in the $Sur2^{+/-}$ or $Sur2^{-/-}$ mice from their wild-type littermates.

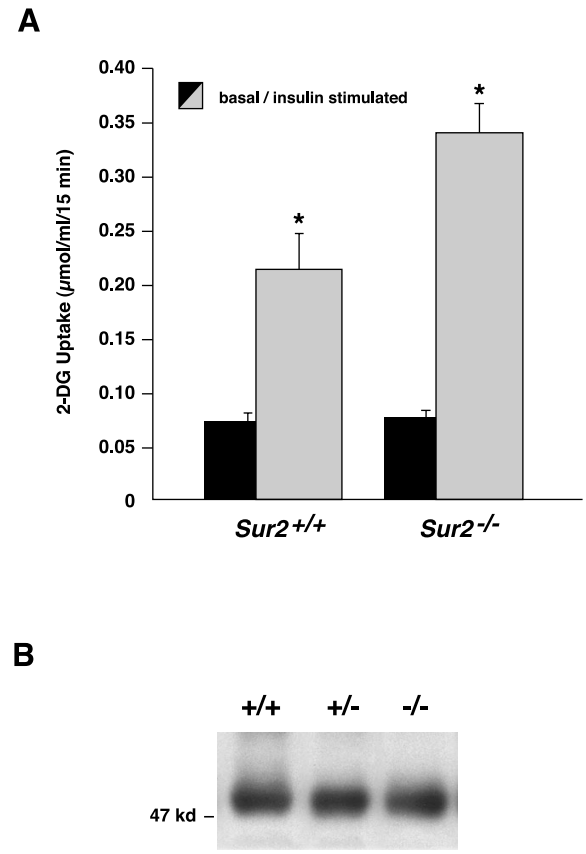

Fig. 3. (*A*) *In vitro* 2-[^{14}C]deoxyglucose uptake into the soleus muscle of male $Sur2^{+/+}$ and $Sur2^{-/-}$ mice. Soleus muscles were incubated in the absence of insulin (basal transport) or high insulin (2,000 microunits/ml) before and during transport study. Bars represent mean ± SEM, $n = 5$, for each group. *, $P < 0.04$ vs. $Sur2^{+/+}$ mice. (*B*) Representative Western blot of hindlimb skeletal muscle of $Sur2^{+/+}$, $Sur2^{+/-}$, and $Sur2^{-/-}$ mice. The microsomal fraction was separated by SDS/PAGE and probed with anti-GLUT4 antiserum. 2-DG, 2-[^{3}H]deoxyglucose.

Discussion

We demonstrated that eliminating muscle K_{ATP} channel currents in mice by disrupting *Sur2* results in increased insulin responsiveness in skeletal muscle. Because SUR2 is not expressed in pancreatic tissue, it is not surprising that gross pancreatic function is undisturbed in this model, as evidenced by the normal fasting and fed insulin levels and unaltered islet architecture of $Sur2^{-/-}$ mice (islet histology not shown). Furthermore, basal glucose homeostasis is minimally affected with only small albeit significant decreases in baseline serum glucose concentration. The role of the skeletal muscle K_{ATP} channel then, and likely membrane excitability, represents an intriguing facet of the insulin-signaling pathway. Early postreceptor signaling steps in insulin action have been established and include increases in phosphorylation of insulin receptors and substrates that lead to a rapid increase in glucose uptake (21). Late steps have also been studied extensively and involve translocation of glucose transporters (GLUT4) from subcellular vesicle stores to the sarcolemma, with vesicle fusion increasing membrane permeability to glucose (22). The intermediate steps are less well understood. One well-characterized postinsulin/receptor binding event is the activation of the Na/K-ATPase cotransporter, which leads to a hyperpolarization of the membrane (23). Increased Na/K-ATPase activity has been associated with an increase in glycolytic flux by increasing the supply of ADP necessary for early steps in glucose metabolism (26).

The role of changes in membrane potential regarding insulin action is not clearly defined. Insulin treatment of skeletal muscle has long been known to hyperpolarize the skeletal muscle membrane (25–27), and insulin-induced hyperpolarization has been proposed as a transducing mechanism mediating insulin action (28, 29). Supporting this hypothesis, artificial hyperpolarization of skeletal muscle has been shown to stimulate glucose uptake (30). In addition, insulin opens K_{ATP} channels, which would also lead to increased skeletal muscle hyperpolarization (31), possibly implicating K_{ATP} as a component of insulin-induced hyperpolarization.

In contrast, past reports suggest that inhibiting K_{ATP} channels with sulfonylureas, which should lead to cell membrane depolarization, also enhances insulin-stimulated glucose uptake, whereas K_{ATP} channel openers inhibit the effect (32–37). The seemingly contradicting evidence between this mechanism and insulin-induced hyperpolarization underscores a complex series of excitation events occurring at the skeletal muscle membrane after insulin binds to its receptor. Zierler and Wu (38) reported that insulin-induced hyperpolarization was the consequence of a reduction in both potassium and sodium permeability—the greater relative diminishment in sodium permeability, such that $P_K > P_{Na}$, leads to hyperpolarization. It has also been proposed

PHYSIOLOGY

that K_{ATP} channels mediate the efflux of potassium after stimulation of the Na/K-ATPase (39). The K_{ATP} channel role certainly might not reflect an initial signaling event, but it may involve subsequent steps such as restoring the resting membrane potential. Thus, an initial hyperpolarization, whether through activation of the Na/K-ATPase or via other mechanisms, may be important in initiating a sequence of events leading to increased glucose transport, whereas opening the K_{ATP} channel results in termination of the signal. In the absence of insulin, then, little effect of the disruption of the K_{ATP} channel should be seen, which is consistent with the normal basal glucose uptake in our isolated muscle transport studies, and enhanced transport after insulin stimulation. Also consistent are our *in vivo* observations that only a small decrease in basal glucose levels are seen, but a marked and increasing rate of glucose infusion is needed to maintain a target blood glucose level for the $Sur2^{-/-}$ mice during a hyperinsulinemic-euglycemic clamp (Fig. 2*C*). These observations suggest that eliminating the muscle K_{ATP} channel results in a defect in dissipation of the insulin signal.

Although we demonstrated a defect intrinsic to the skeletal muscle, it is also possible that alterations in vascular flow caused by an absence in vascular smooth muscle K_{ATP} current affect glucose delivery to skeletal muscle. Indeed, increases in blood flow have been shown to correlate with insulin-mediated glucose uptake (40), and it has been suggested that insulin directly induces vasodilatation, perhaps through an NO-mediated event (41). Although we have detected a significant elevation of blood pressure in the $Sur2^{-/-}$ mice (W.A.C., J.P., J.C.M., C.F.B., and E. McNally, unpublished work), insulin-mediated vasodilatation may still occur and perhaps be enhanced because of the disruption of K_{ATP}.

In summary, the SUR2 K_{ATP} channel apparently is important for regulation of insulin signaling in skeletal muscle. These findings shed light on the observations of Kir6.2 null mice, which lack both β cell K_{ATP} and skeletal muscle K_{ATP} (11). The enhanced peripheral insulin responsiveness demonstrated in the absence of extra-pancreatic K_{ATP} can provide a direct account for the survival of Kir6.2 null mice, despite their significantly reduced circulating insulin levels and blunted β cell response. Our findings also suggest a mechanism for the small enhancement of insulin action in the periphery by sulfonylureas. Because the sulfonyureas have up to a 100-fold lower affinity for SUR2-containing potassium channels as for the SUR1-containing channels (42), it may be possible to design specific high-affinity inhibitors of this channel that could allow enhanced insulin action. In addition, studies focusing on membrane excitability and its function in insulin action may provide a key link between early postinsulin signaling events and the late events that result in GLUT4 vesicle translocation and increased glucose transport.

We thank Jon Davison for his technical contributions to the *in vitro* glucose transport studies and Kevin Galles for his technical work in breeding mice and isolating cardiac myocytes. We also thank Linda Degenstein for her expert technical work in stem cell/blastocyst injection and the generation of the transgenic animals. We are grateful to Drs. Graeme Bell, Lou Philipson, and Donald Steiner for critically reading drafts of this manuscript. Finally, we thank Dr. Kenneth Polonsky for his support toward initiating this project and the generation of the knockout mice. This work was supported by funding from the National Institutes of Heath Grants DK-KO8-02170 (C.F.B.) and RO1 HL-57414 (J.C.M.), and the Oscar Rennebohm Foundation (J.C.M.).

1. Chutkow, W. A., Simon, M. C., Le Beau, M. M. & Burant, C. F. (1996) *Diabetes* **45,** 1439–1445.
2. Seino, S. (1999) *Annu. Rev. Physiol.* **61,** 337–362.
3. Clement, J. P. t., Kunjilwar, K., Gonzalez, G., Schwanstecher, M., Panten, U., Aguilar-Bryan, L. & Bryan, J. (1997) *Neuron* **18,** 827–838.
4. Inagaki, N., Gonoi, T., Clement, J. P. t., Namba, N., Inazawa, J., Gonzalez, G., Aguilar-Bryan, L., Seino, S. & Bryan, J. (1995) *Science* **270,** 1166–1170.
5. Chutkow, W. A., Makielski, J. C., Nelson, D. J., Burant, C. F. & Fan, Z. (1999) *J. Biol. Chem.* **274,** 13656–13665.
6. Shindo, T., Yamada, M., Isomoto, S., Horio, Y. & Kurachi, Y. (1998) *Br. J. Pharmacol.* **124,** 985–991.
7. Gross, G. J. (2000) *Basic Res. Cardiol.* **95,** 280–284.
8. Grover, G. J. (1997) *Can. J. Physiol. Pharmacol.* **75,** 309–315.
9. Gross, G. J. (1995) *Basic Res. Cardiol.* **90,** 85–88.
10. Pang, C. Y., Neligan, P., Xu, H., He, W., Zhong, A., Hopper, R. & Forrest, C. R. (1997) *Am. J. Physiol.* **273,** H44–H51.
11. Miki, T., Nagashima, K., Tashiro, F., Kotake, K., Yoshitomi, H., Tamamoto, A., Gonoi, T., Iwanaga, T., Miyazaki, J. & Seino, S. (1998) *Proc. Natl. Acad. Sci. USA* **95,** 10402–10406.
12. Tybulewicz, V. L., Crawford, C. E., Jackson, P. K., Bronson, R. T. & Mulligan, R. C. (1991) *Cell* **65,** 1153–1163.
13. Bradley, A. & Robertson, E. (1986) *Curr. Top. Dev. Biol.* **20,** 357–371.
14. Sambrook, J., Fritsch, E. F. & Maniatis, T. (1989) *Molecular Cloning: A Laboratory Manual* (Cold Spring Harbor Lab. Press, Plainview, NY), 2nd Ed.
15. Ohlendieck, K., Ervasti, J. M., Snook, J. B. & Campbell, K. P. (1991) *J. Cell Biol.* **112,** 135–148.
16. Pi, Y., Sreekumar, R., Huang, X. & Walker, J. W. (1997) *Circ. Res.* **81,** 92–100.
17. Kim, J. K., Michael, M. D., Previs, S. F., Peroni, O. D., Mauvais-Jarvis, F., Neschen, S., Kahn, B. B., Kahn, C. R. & Shulman, G. I. (2000) *J. Clin. Invest.* **105,** 1791–1797.
18. Hansen, P. A., Gulve, E. A., Marshall, B. A., Gao, J., Pessin, J. E., Holloszy, J. O. & Mueckler, M. (1995) *J. Biol. Chem.* **270,** 1679–1684.
19. Young, D. A., Uhl, J. J., Cartee, G. D. & Holloszy, J. O. (1986) *J. Biol. Chem.* **261,** 16049–16053.
20. Isomoto, S., Kondo, C., Yamada, M., Matsumoto, S., Higashiguchi, O., Horio, Y., Matsuzawa, Y. & Kurachi, Y. (1996) *J. Biol. Chem.* **271,** 24321–24324.
21. Virkamaki, A., Ueki, K. & Kahn, C. R. (1999) *J. Clin. Invest.* **103,** 931–943.
22. St-Denis, J. F. & Cushman, S. W. (1998) *J. Basic Clin. Physiol. Pharmacol.* **9,** 153–165.
23. Sweeney, G. & Klip, A. (1998) *Mol. Cell. Biochem* **182,** 121–133.
24. James, J. H., Fang, C. H., Schrantz, S. J., Hasselgren, P. O., Paul, R. J. & Fischer, J. E. (1996) *J. Clin. Invest.* **98,** 2388–2397.
25. Flatman, J. A. & Clausen, T. (1979) *Nature (London)* **281,** 580–581.
26. Moore, R. D. & Rabovsky, J. L. (1979) *Am. J. Physiol.* **236,** C249–C254.
27. Otsuka, M. & Ohtsuki, I. (1965) *Nature (London)* **207,** 300–301.
28. Zierler, K. & Rogus, E. M. (1981) *Biochim. Biophys. Acta* **640,** 687–692.
29. Zierler, K., Rogus, E. M., Scherer, R. W. & Wu, F. S. (1985) *Am. J. Physiol.* **249,** E17–E25.
30. Zierler, K. & Rogus, E. M. (1980) *Am. J. Physiol.* **239,** E21–E29.
31. Tricarico, D., Mallamaci, R., Barbieri, M. & Conte Camerino, D. (1997) *Biochem. Biophys. Res. Commun.* **232,** 536–539.
32. Bak, J. F., Schmitz, O., Sorensen, N. S. & Pedersen, O. (1989) *Diabetes* **38,** 1343–1350.
33. Salhanick, A. I., Konowitz, P. & Amatruda, J. M. (1983) *Diabetes* **32,** 206–212.
34. Kern, M., Loomis, T. A., Tapscott, E. B. & Dohm, G. L. (1993) *Int. J. Biochem.* **25,** 1257–1261.
35. Wang, P. H., Moller, D., Flier, J. S., Nayak, R. C. & Smith, R. J. (1989) *J. Clin. Invest.* **84,** 62–67.
36. Vestergaard, H., Weinreb, J. E., Rosen, A. S., Bjorbaek, C., Hansen, L., Pedersen, O. & Kahn, B. B. (1995) *J. Clin. Endocrinol. Metab.* **80,** 270–275.
37. Greenfield, M. S., Doberne, L., Rosenthal, M., Schulz, B., Widstrom, A. & Reaven, G. M. (1982) *Diabetes* **31,** 307–312.
38. Zierler, K. & Wu, F. S. (1988) *Trans. Assoc. Am. Physicians* **101,** 320–325.
39. Tricarico, D., Servidei, S., Tonali, P., Jurkat-Rott, K. & Camerino, D. C. (1999) *J. Clin. Invest.* **103,** 675–682.
40. Baron, A. D., Steinberg, H., Brechtel, G. & Johnson, A. (1994) *Am. J. Physiol.* **266,** E248–E253.
41. Baron, A. D., Tarshoby, M., Hook, G., Lazaridis, E. N., Cronin, J., Johnson, A. & Steinberg, H. O. (2000) *Diabetes* **49,** 768–774.
42. Inagaki, N., Gonoi, T., Clement, J. P., Wang, C. Z., Aguilar-Bryan, L., Bryan, J. & Seino, S. (1996) *Neuron* **16,** 1011–1017.